HHS Public Access

Author manuscript

*Am J Sports Med*. Author manuscript; available in PMC 2019 July 01.

Published in final edited form as:

*Am J Sports Med*. 2018 July ; 46(9): 2161–2169. doi:10.1177/0363546518769267.

# Fatty Infiltration Is a Prognostic Marker of Muscle Function After Rotator Cuff Tear

**Ana P. Valencia, PhD**[*,†], **Jim K. Lai, MD**[*], **Shama R. Iyer, PhD**[*], **Katherine L. Mistretta, BS**[*], **Espen E. Spangenburg, PhD**[‡], **Derik L. Davis, MD**[§], **Richard M. Lovering, PT, PhD**[*,‖], **Mohit N. Gilotra, MD**[*,¶,#], and **Investigation performed at the Department of Orthopaedics, University of Maryland School of Medicine, Baltimore, Maryland, USA, and the Baltimore Veteran Affairs Medical Center, Baltimore, Maryland, USA**

[*]Department of Orthopaedics, School of Medicine, University of Maryland, Baltimore, Maryland, USA

[†]Department of Kinesiology, School of Public Health, University of Maryland, Baltimore, Maryland, USA

[‡]Department of Physiology, East Carolina Diabetes and Obesity Institute, Brody School of Medicine, East Carolina University, Greenville, North Carolina, USA

[§]Department of Diagnostic Radiology and Nuclear Medicine, School of Medicine, University of Maryland, Baltimore, Maryland, USA

[‖]Department of Physiology, School of Medicine, University of Maryland, Baltimore, Maryland, USA

[¶]Department of Orthopaedics, Baltimore Veteran Affairs Medical Center, Baltimore, Maryland, USA

## Abstract

**Background:** Massive rotator cuff tears (RCTs) begin as primary tendon injuries and cause a myriad of changes in the muscle, including atrophy, fatty infiltration (FI), and fibrosis. However, it is unclear which changes are most closely associated with muscle function.

**Purpose:** To determine if FI of the supraspinatus muscle after acute RCT relates to short-term changes in muscle function.

**Study Design:** Controlled laboratory study.

**Methods:** Unilateral RCTs were induced in female rabbits via tenotomy of the supraspinatus and infraspinatus. Maximal isometric force and rate of fatigue were measured in the supraspinatus in vivo at 6 and 12 weeks after tenotomy. Computed tomography scanning was performed, followed by histologic analysis of myofiber size, FI, and fibrosis.

[#]Address correspondence to Mohit N. Gilotra, MD, Department of Orthopaedics, School of Medicine and VA Maryland Health Care System, University of Maryland, AHB, Rm 540, 100 Penn St, Baltimore, MD 21201, USA (mgilotra@som.umaryland.edu).

One or more of the authors has declared the following potential conflict of interest

**Results:** Tenotomy resulted in supraspinatus weakness, reduced myofiber size, FI, and fibrosis, but no differences were evident between 6 and 12 weeks after tenotomy except for increased collagen content at 12 weeks. FI was a predictor of supraspinatus weakness and was strongly correlated to force, even after accounting for muscle cross-sectional area. While muscle atrophy accounted for the loss in force in tenotomized muscles with minimal FI, it did not account for the greater loss in force in tenotomized muscles with the most FI. Collagen content was not strongly correlated with maximal isometric force, even when normalized to muscle size.

**Conclusion:** After RCT, muscle atrophy results in the loss of contractile force from the supraspinatus, but exacerbated weakness is observed with increased FI. Therefore, the level of FI can help predict contractile function of torn rotator cuff muscles.

**Clinical Relevance:** Markers to predict contractile function of RCTs will help determine the appropriate treatment to improve functional recovery after RCTs.

### Keywords

Supraspinatus; muscle force; muscle fatty infiltration; muscle atrophy; rotator cuff; animal model

Rotator cuff (RC) muscles undergo a variety changes after tendon tear, including atrophy, fibrosis, and fatty infiltration (FI), which prevent full recovery of shoulder function.[12,48] In addition, these muscle changes predict RC retear after repair.[23] Current therapies to improve functional outcomes after massive rotator cuff tears (RCTs) focus on tendon-to-bone healing but show limited success.[32,44,58] New strategies are focused on decreasing or reversing muscle atrophy, fibrosis, or FI,[18,26,49] but it is unclear if these changes contribute equally or even codependently to RC muscle function.

Relatively few studies have assessed physiological function in torn RC muscles,[13,16,39] and none have assessed the relationship of muscle force production to histological changes in the muscle, such as fibrosis, myofiber size, or intramuscular adipocyte accumulation. For patients, functional testing of RC muscles is difficult since the muscles cannot be isolated for testing,[33] and for animals, it is difficult to access RC muscles deep to the deltoid and acromion in vivo. Most studies suggest that RC muscle weakness is largely related to muscle cross-sectional area (CSA)[19,39]; however, with RCTs, the muscle undergoes numerous cellular changes beyond a decrease in size that could influence muscle force production.[20,50]

The objective of the study was to determine if a relationship exists between histological changes and decreases in muscle function in the RC muscles after an acute tear. We hypothesized that the amount of supraspinatus FI would best predict a loss in muscle function. To mimic the human condition, we utilized a large rabbit rotator cuff tenotomy model[45] and assessed histological and physiological outcomes 6 and 12 weeks after the onset of the tear.[46]

## METHODS

### Animals

All protocols were approved by the University of Maryland Institutional Animal Care and Use Committee. We used skeletally mature New Zealand White rabbits (body weight, 2.3

± 0.6 kg; Charles River Laboratories). Animals were randomly selected to serve as controls (intact RC) or undergo unilateral tenotomy. Samples were not subject to all outcome measures. Supraspinatus contractile testing was performed in 18 rabbits representing 3 experimental groups (control and after 6 and 12 weeks of tenotomy). According to our preliminary data, a sample size of 4 rabbits per group was sufficient to show a significant difference in contractile force. The power calculation was based on a minimal detectable difference of 2.295 N, with an expected 0.86 SD of residuals, for a desired power of 0.8 and alpha value of .05, based on previously published data.[57] Twelve rabbits completed both contractile testing and histology, which were used for correlational and regression analyses retrospectively.

### Tenotomy

A 2-cm incision was introduced just distal to the acromion process. The deltoid was reflected posteriorly, and the supraspinatus and infraspinatus tendons were identified, transected, and sutured with a 5–0 Prolene (Ethicon) to a Penrose drain (Grafco) to prevent spontaneous adhesions, as done previously.[45]

### Contractile Function

Contractile function of the isolated supraspinatus muscle was measured in anesthetized animals as described previously.[57] Briefly, the tendon of the supraspinatus muscle was released and attached to a load cell. The suprascapular nerve was stimulated via subcutaneous needle electrodes (J05 Needle Electrode Needles, 36BTP; Jari Electrode Supply) placed at the suprascapular notch. Single twitches (rectangular pulse, 1 millisecond) were applied at different muscle lengths to determine the optimal length (resting length, $L_0$). At $L_0$, maximally fused tetanic contraction was obtained at ~100 Hz (300-millisecond train duration of 1-millisecond pulses at a constant current of 5 mA). We used 150% of the maximal stimulation intensity to induce maximal activation of contraction, $P_0$. A force-frequency plot was generated for each muscle, obtained by progressively increasing the frequency of pulses during a 200-millisecond pulse train. To provide an index of fatigue, maximal tetanic contractions were performed repeatedly (every 2 seconds) for 2 minutes, with the final tension expressed as percentage of $P_0$. Although contractile testing was performed in vivo, the animal was euthanized after the procedure, and the shoulder girdles were harvested.

### Micro–Computed Tomography Imaging

After euthanasia, the shoulder girdle of 12 animals was harvested to undergo micro–computed tomography scanning (86-mm resolution, 55 kV, 200 mA; Inveon CT, Siemens Medical Solutions USA). Hounsfield unit calibration was performed with a custom-made double-distilled water phantom. Images were reconstructed for a slice thickness of 172 mm with beam-hardening correction. The Y-shape view obtained from the computed tomography sagittal oblique imaging plane was analyzed with Aquarius iNtuition Edition software (v 4.4; TeraRecon Inc) to quantify the CSA ($cm^2$) of the supraspinatus muscle. Measurements were performed in a blinded fashion by a licensed and board-certified musculoskeletal radiologist.

### Fatty Infiltration

Fixed supraspinatus muscles (4% paraformaldehyde) were used to make paraffin-embedded cross sections along the muscle belly. Sections were stained with hematoxylin and eosin (H&E) and viewed under a brightfield microscope (Nikon Eclipse 50i). A sequence of ~300 adjacent images was captured with a high-resolution color camera (Nikon DS-Fi2) with a 203 objective. The images were electronically stitched to create a high-magnification mosaic of the entire cross section of the muscle belly (NIS Elements Viewer) (Appendix 1, available in the online version of this article). Stitched images were then analyzed on ImageJ (National Institutes of Health) to assess FI. The image was converted to an 8-bit grayscale, and the total stained area ($mean_{TSA}$) was selected with thresholds to obtain the mean gray value. Adipocytes in the peri- and intrafascicular spaces were identified with a previously defined method.[20] Briefly, non-eosin-stained cells that reside within the fascicle inside the perimysium border were identified as intrafascicular adipocytes, and non-eosin-stained cells located between fascicles were identified as perifascicular adipocytes. The area covered with adipocytes was manually identified, and the mean gray value was obtained for the total stained area plus adipocytes ($mean_{TSA1A}$). Percentage area covered by adipocytes, which we refer to as *percentage FI*, was calculated by ($mean_{TSA1A} - mean_{TSA}$) / $mean_{TSA}$ multiplied by 100.

### Immunolabeling

Paraffin-embedded sections were deparaffinized through a 1-hour heating period (65°C), followed by a 10-minute incubation in boiling sodium citrate buffer (10mM sodium citrate, 0.05% Tween 20, pH 6.0) and xylene washes. The sections were rehydrated in decreasing ethanol solutions and washed in phosphate-buffered saline. Sections were incubated overnight at 4°C in a 1:50 dilution of perilipin 1 antibody (kindly provided by Dr Carole Sztalryd, University of Maryland, Baltimore), an adipocyte-specific protein. Sections were then incubated in a 1:100 dilution with secondary antibodies conjugated with Alexa 488 (Invitrogen) and visualized with a fluorescent microscope (Nikon Eclipse 50i).

### Feret Diameter

Stitched images taken at 203 magnification of H&Estained sections were also used to calculate myofiber size. Myofibers (100 per animal) were selected at random across the whole section for each muscle and manually outlined to calculate minimal Feret diameter with ImageJ. Minimal Feret diameter is the minimum distance between parallel tangents at opposing borders of the myofiber and is a valid measurement of myofiber size.[4] The mean Feret diameter per group was calculated, as well as the mean distribution of fibers according to their diameter.

### Collagen Content

Paraffin-embedded sections were deparaffinized in xylene, rehydrated, stained for 1 hour with Picrosiriusred (0.1% Direct Red saturated in aqueous picric acid; Sigma), and rinsed with acidified water (5% acetic acid). As done for H&E images, a sequence of adjacent images of stained sections was similarly captured (Appendix 1). Stitched images were then analyzed on ImageJ. To assess the area of collagen of the entire section, the background was

subtracted, and thresholds were used to determine the total stained area of the section ($mean_{TSA}$). Another threshold was used to include only the area stained red (collagen) ($mean_{col}$). To calculate percentage area stained with Picrosirius red, the $mean_{col}$ was divided by $mean_{TSA}$ and multiplied by 100.

### Statistical Analysis

Normality and homogeneity of variance were verified for all data before analysis (SigmaStat). To evaluate potential differences among the 3 groups, a 1-way analysis of variance was used, followed by a post hoc Holm-Sidak test when the analysis was significant. Significance was set at $P < .05$, and data are represented as mean ± SD. Normality was not met for the histological assessment of percentage FI, as values for control muscles were close to the zero limit, skewing the data to the left. A Kruskal-Wallis test was used to compare percentage FI among the 3 groups, followed by a post hoc Dunn test when the Kruskal-Wallis test was significant to determine differences in percentage FI among groups. Pearson correlation coefficients were calculated in the subset of muscles that underwent histological analysis and contractile testing to determine the association between maximal isometric force and histological markers. Histological markers were entered as independent variables in a stepwise multiple linear regression analysis, with maximal isometric force set as the dependent variable.

## RESULTS

There was a 40% to 45% reduction in maximal contractile force in the supraspinatus muscle after 6 weeks ($P = .004$) and 12 weeks ($P = .003$) of tenotomy as compared with control (16.1 ± 1.7 N) (Figure 1A). However, maximal contractile force was not different between 6 and 12 weeks (9.6 ± 3.2 N vs 8.8 ± 5.7 N, $P = .713$). The amount of developed muscle fatigue, as evidenced by a loss in force output after a repetitive stimulation protocol, was not different among the groups (–45.4% ± 4.7%, $P = .867$; Figure 1B).

Histological analysis of the supraspinatus at 6 and 12 weeks after tenotomy showed FI, as evidenced by the presence of intramuscular adipocytes and confirmed with perilipin 1 (Figure 2A, green). Adipocytes covered 7% ± 6% (6 weeks) and 12% ± 7% (12 weeks) of the tissue sections stained with H&E but were negligible in the control (0.3% ± 0.2%) (Figure 2B, bar graph). No difference in FI was evident between 6 and 12 weeks ($P = .853$). In tenotomized muscles, the greatest proportion of adipocytes (79% ± 15%) was in the perifascicular spaces, specifically closer to blood vessels, with a smaller proportion of adipocytes (18% ± 14%) in the intrafascicular space (Figure 2B, bottom).

The distribution of myofiber diameter showed a shift toward smaller muscle fibers at both time points after tenotomy (Figure 3A) as compared with the control muscle. The mean myofiber diameter was 22% lower after 6 weeks and 24% lower after 12 weeks versus control (56.7 ± 3.1 mm, $P = .0005$; Figure 3B), with no differences evident between 6 and 12 weeks ($P = .671$).

Fibrosis was evident only after 12 weeks of tenotomy, as evidenced by an increased Picrosirius red staining of the supraspinatus muscle as compared with the control group (18% ± 7% vs 6% ± 4%, $P = .004$) (Figure 4).

The histological markers for FI, fibrosis, and myofiber size were all correlated to maximal tetanic force (Figure 5A). However, the marker for FI (percentage area covered by adipocytes) had the strongest correlation with muscle force ($R = 0.819$, $P = .001$) and was the only predicting factor of muscle force when the 3 histological markers were incorporated into a stepwise multiple linear regression model ($P = .016$) (Figure 5B). To better delineate the characteristics determining supraspinatus force, muscles were divided into thirds according to muscle force generated. Muscles with force values in the top third (17 ± 1.2 N) were grouped into the strongest group; muscles with force values in the middle third (12.3 ± 1.8 N), the weak group; and muscles with force values in the bottom third (5.9 ± 1.4 N), the weakest group (Figure 5C). The strongest group consisted of only intact control muscles, while the weak and weakest groups included tenotomized muscles of the 6- and 12-week time points. Compared with the strongest muscles, where there was close to no FI, weaker muscles had FI (3.3% ± 2.3%), but the percentage area covered by myofibers was not significantly different (85.8% ± 3.6%, $P = .115$). The weakest muscles had the most FI (13.5% ± 7.0%, $P = .033$) and a decreased percentage area covered by myofibers (71.8% ± 9.5%, $P = .001$ vs strongest, $P = .010$ vs weak). When the location of FI between the weak and weakest groups was compared, there was more FI in the perifascicular space in the weakest group ($P = .025$) but no significant difference in the intrafascicular space ($P = .077$).

CSA of the supraspinatus muscle belly was measured with micro–computed tomography (Figure 6A, top). CSA was smaller than control (1.16 ± 0.31 $cm^2$) at 6 weeks (0.567 ± 0.13 $cm^2$, $P = .004$) and 12 weeks (0.757 ± 0.19 $cm^2$, $P = .025$) after tenotomy but not different between the time points after tenotomy ($P = .2$) (Figure 6A, bottom). Lower muscle density (in Hounsfield units) corresponded with percentage FI obtained from histology (Appendix 2, available online). The mean CSA for each group was used to estimate the total area covered by collagen, fat, and myofibers in the supraspinatus muscle by multiplying it with the proportions of collagen, fat, and myofibers previously calculated through histology.

Since the duration of the tear did not have a significant effect on force, size, or composition of the muscle, we further examined the characteristics of muscles according to maximal force generated (Figure 6B). Compared with the strongest group, the weak group had a smaller total area covered by myofibers (0.53 ± 0.07 $cm^2$, $P = .0003$) that accounted for the difference in muscle force, but the area covered by myofibers in the weakest group was not significantly different from the weak group (0.44 ± 0.03 $cm^2$, $P = .284$) despite a significant reduction in force ($P = .0002$). The degree of FI was not different between the strongest and weak groups ($P = .492$). In contrast, the weakest group had a significant level of FI (0.09 ± 0.05 $cm^2$, $P = .0216$ vs weak, $P = .007$ vs strongest). There was no difference in centrally nucleated fibers among groups (Appendix 3, available online).

## DISCUSSION

The supraspinatus muscle undergoes a variety of changes after RCT[17,20,23] that impair functional recovery, such as atrophy, FI, and fibrosis; however, it is unclear if these changes contribute equally or disproportionately to changes in RC muscle function. Our findings show that supraspinatus atrophy and FI are strongly correlated with loss in contractile force after an acute RCT, but the weakest tenotomized muscles were characterized by marked FI rather than worsening atrophy. Our findings support various studies that showed increased FI and fibrosis and a decrease in myofiber size in tenotomized RC muscles,[31,46,47] but this study is the first to associate these factors with muscle force and, to the best of our knowledge, the first to provide a histological marker as a surrogate for contractile function.

The influence of RC muscle weakness on shoulder dysfunction has been documented.[29,52] The force loss of RC muscles destabilizes the glenohumeral joint[29] and results in unwanted contact between the humerus and acromion.[51] Therefore, improvement in shoulder function after RCT depends on not only proper reattachment of the tendon but also the ability of the repaired muscle to generate force.[40] The forces generated by RC muscles may provide the mechanical load necessary for optimal tendon healing after repair.[2,30] Functional recovery after RCT therefore depends on the restitution of normal muscle structure and function.[40]

The decision to undergo RC repair is based on pain, age, tear, and degree of atrophy and FI in the muscle.[14] Muscle atrophy can improve after repair,[15,56] but FI does not.[23,27] In addition, degenerative muscle findings can predict RCT.[23] While the amount of atrophy is generally used to estimate the contractile capacity of muscle,[40] atrophied muscles after RCT have varying degrees of FI. A muscle with atrophy but little FI is more likely to be stronger than an atrophied muscle with significant FI and therefore more likely to have improved function after repair, especially if muscle mass improves after repair and rehabilitation. These concepts can help guide clinicians in the surgical and rehabilitation planning after RCT. Furthermore, defining the molecular pathways that lead to FI would provide attractive targets for future therapeutic interventions.

Fibrosis of the supraspinatus was not a strong influence on muscle force. This was unanticipated, as the extracellular matrix contributes to skeletal muscle structure, mechanical properties,[21,36] transduction of mechanical force, and muscle remodeling.[42] Gradual deposition of extracellular matrix proteins in the muscle is common in muscle injury and can increase up to 10-fold in injured muscle.[36] The role of fibrosis on RCTs is still unclear, as fibrosis was evident in some studies with animal models of RCT[24,37] and not in others.[47,50] Antifibrotic drugs improve muscle histologic properties and even muscle function in rodent models,[9,25] but the effect of these drugs may be on fibrosis and fat, especially when targeting fibroadipogenic cells.[8] Fibrosis may also increase myofiber injury risk[10] and the repair tension necessary to reattach the muscle to the humeral head.[22]

In healthy muscle, muscle mass is the strongest predictor of muscle force, but atrophy did not fully account for the loss in force in tenotomized muscles with the most FI. In other words, the difference between the weak and weakest tenotomized muscles was not explained by a loss in myofibers or CSA but rather by an increase in the amount of FI. Myofiber

degeneration can promote the differentiation of muscle-resident stem cells into adipocytes[28,35] by blocking the Rho signaling pathway.[5,28] The close proximity of adipocytes and myofibers in muscles with FI can also impair muscle function, as adipocytes can reduce the expression of contractile and structural proteins,[43] promote myofiber atrophy, and disrupt muscle regeneration.[7,43,53] Adipocytes secrete fatty acids, adipokines, cytokines, and chemokines like IL-1b58 that promote inflammation[43] and induce oxidative stress,[6] which can further reduce force generating capacity of myofibers.[1,34] Indeed, the presence of FI could explain the significant force reduction in the weakest cohort.[42] The location of the adipocytes in relation to myofibers likely matters as well. Perifascicular adipocytes are more likely to affect adjacent myofibers as compared with adipocytes inside the perimysium.

There are currently no effective treatments used to prevent or reduce FI after RCT. To reduce FI, the source of adipocytes should be understood. After tenotomy, there was a greater concentration of adipocytes in the perifascicular space, specifically near vascular walls, as also documented in RC muscles from patients with RCTs.[20] The significance of finding adipocytes close to vascular walls is that a number of muscle progenitor cells (ie, fibroadipogenic cells, pericytes, myogenic endothelial cells) reside in the same location and contribute to muscle development and regeneration[11,41,60] but, in some cases, can differentiate into intramuscular adipocytes.[3,59] H&E staining is commonly used to identify adipocytes in muscle, which have a characteristic ovoid shape surrounded by a rim of cytoplasm. Because identification relies on negative eosin staining, we confirmed that the cells identified as adipocytes in H&E have an adipocyte-specific marker (perilipin 1). While some suggested the source of FI to be muscleresident progenitor cells,[38] a variety of progenitor cells have not been explored in RC injury.[11,41,59,60]

One potential limitation is that only acute and subacute time points were selected. That is, FI tends to progress over time in the rabbit model of RCT,[46,56] but differences are not always be detected in a time frame 6 weeks.[54,55] Given our findings, neither FI nor contractile force worsened between 6 and 12 weeks, but since FI can progress in a longer time window, muscle force may diminish within that time course as well. It is unclear why some animals developed more FI than others after tenotomy (weak vs weakest), after controlling for tear size, tear duration, sex, and age. One factor may be that the degree of tendon retraction is variable after 2-tendon tenotomy. This may lead to a different amount of FI across both time points. Although we found strong evidence of FI as a predictor of force via histology, more studies are necessary to confirm that FI, as measured by computed tomography, is a reliable predictor of force. Future directions include evaluating FI and muscle function after repair.

## CONCLUSION

The main finding of this study was that FI is a strong indicator of muscle weakness. FI has long been associated with poor outcomes after RCT, and atrophied muscles with significant FI are much weaker than those with atrophy alone.

## Acknowledgments

source of funding: This work was supported by the National Institutes of Health by grants to A.P.V. (T32AG00026815S1), S.R.I. (AR07592-20), and R.M.L. (R01-AR059179 and R21-AR067872). Additional support

to M.N.G. was provided by the Orthopaedic Research and Education Foundation and to M.N.G. and D.L.D. via a pilot grant from VISN-5 (US Department of Veteran Affairs). D.L.D. received a research seed grant (without salary support) in 2016 for an unrelated project from the Radiological Society of North America Research and Education Foundation and Hitachi Medical Systems.

## Appendix

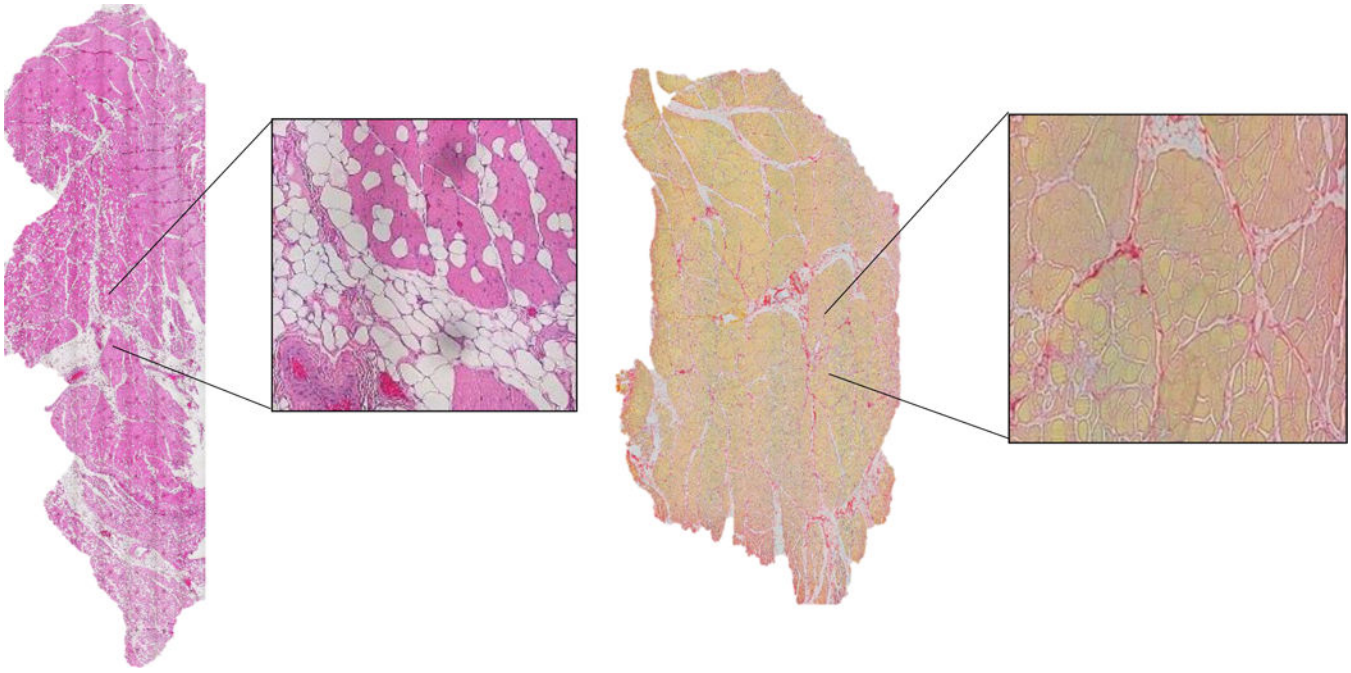

**Appendix Figure A1: Imaging histological sections.**

Stitched mosaic of entire muscle section stained with H&E at 6W (left) or with picrosirius red at 12W (right) imaged at 20x. Insets represent one field of view at 20x.

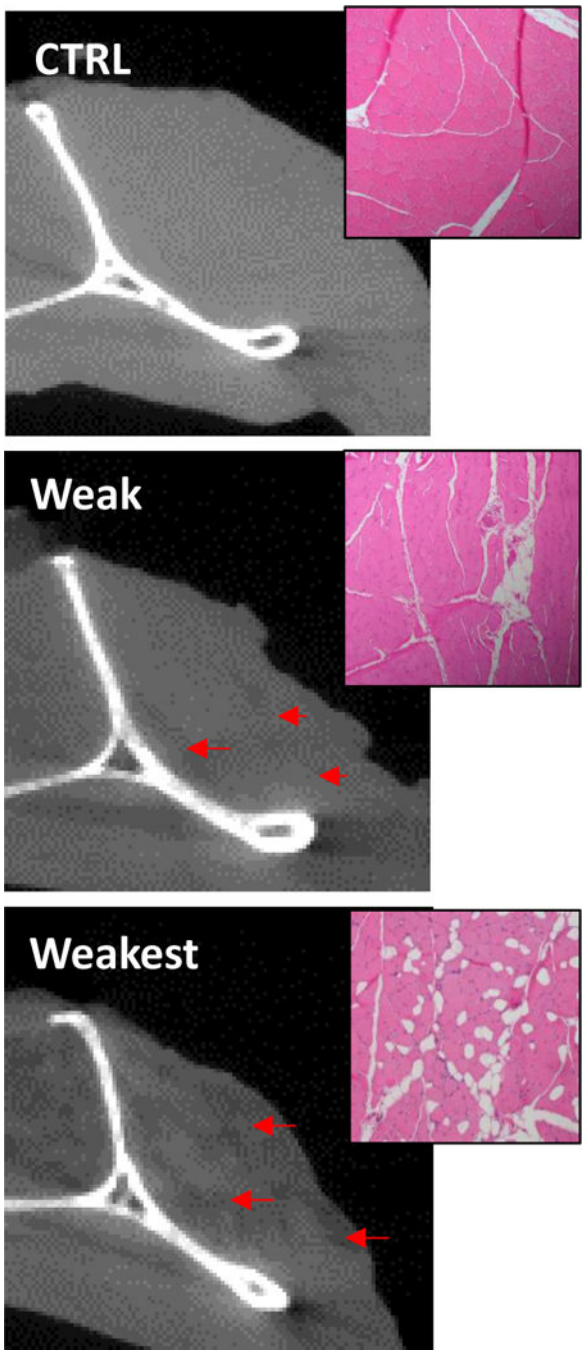


**Appendix Figure A2: FI measured through CT.**
Stitched mosaic of entire muscle section stained with H&E at 6W (left) or with picrosirius red at 12W (right) imaged at 20x. Insets represent one field of view at 20x.

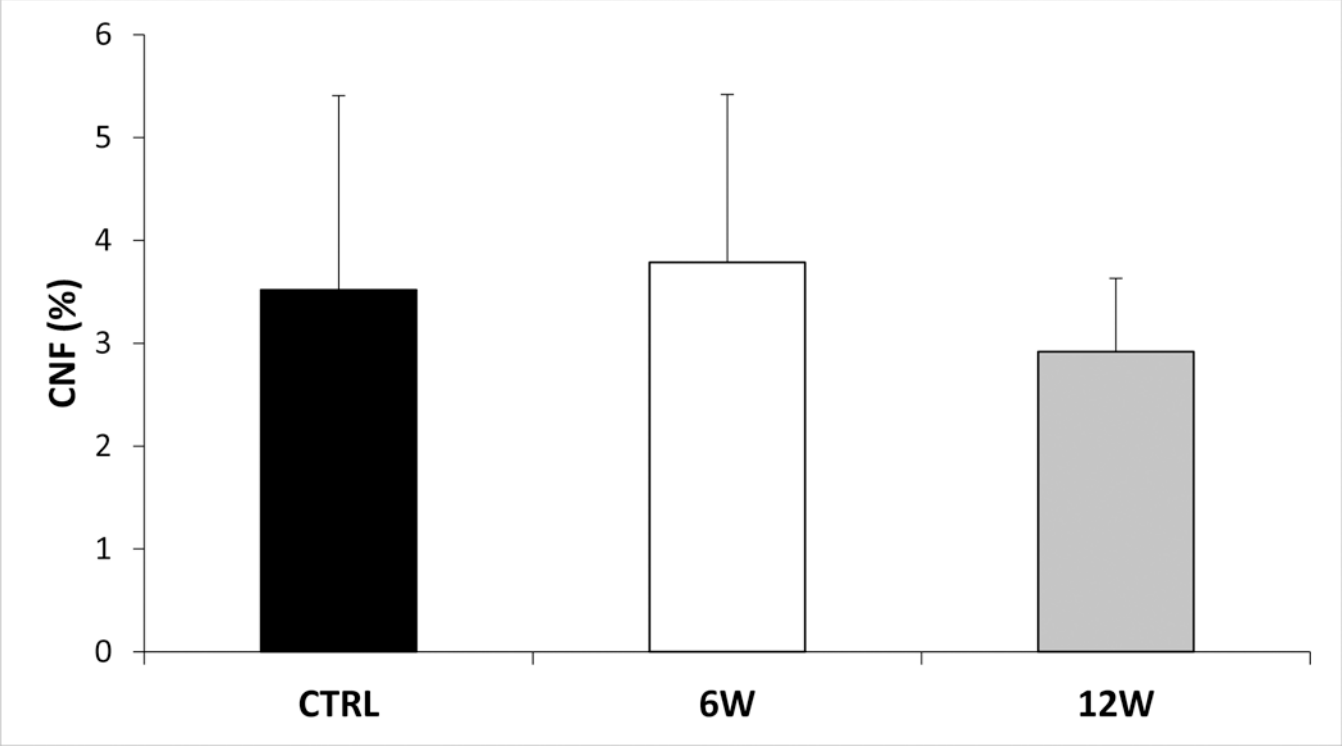


**Appendix Figure A3: Centrally nucleated fibers.**

The percentage of myofibers (out of ~300 myofibers per sample) with nuclei in the cytoplasm were quantified using H&E stained muscle cross sections. CNF, centrally nucleated fibers. All data are presented as mean ± SD.

## REFERENCES

1. Baumann CW, Kwak D, Liu HM, Thompson LV. Age-induced oxidative stress: how does it influence skeletal muscle quantity and quality? J Appl Physiol (1985) 2016;121(5):1047–1052. [PubMed: 27197856]
2. Bayer ML, Yeung CY, Kadler KE, et al. The initiation of embryonic-like collagen fibrillogenesis by adult human tendon fibroblasts when cultured under tension. Biomaterials 2010;31(18):4889–4897. [PubMed: 20356622]
3. Birbrair A, Zhang T, Wang ZM, et al. Role of pericytes in skeletal muscle regeneration and fat accumulation. Stem Cells Dev 2013;22(16): 2298–2314. [PubMed: 23517218]
4. Briguet A, Courdier-Fruh I, Foster M, Meier T, Magyar JP. Histological parameters for the quantitative assessment of muscular dystrophy in the mdx-mouse. Neuromuscul Disord 2004;14(10):675–682. [PubMed: 15351425]
5. Bryan BA, Mitchell DC, Zhao L, et al. Modulation of muscle regeneration, myogenesis, and adipogenesis by the rho family guanine nucleotide exchange factor GEFT. Mol Cell Biol 2005;25(24): 11089–11101. [PubMed: 16314529]
6. Buck M, Chojkier M. Muscle wasting and dedifferentiation induced by oxidative stress in a murine model of cachexia is prevented by inhibitors of nitric oxide synthesis and antioxidants. EMBO J 1996;15(8):1753–1765. [PubMed: 8617220]
7. Choi SH, Chung KY, Johnson BJ, et al. Co-culture of bovine muscle satellite cells with preadipocytes increases PPARgamma and C/EBPbeta gene expression in differentiated myoblasts and increases GPR43 gene expression in adipocytes. J Nutr Biochem 2013;24(3):539–543. [PubMed: 22748806]

8. Davies MR, Liu X, Lee L, et al. TGF-beta small molecule inhibitor SB431542 reduces rotator cuff muscle fibrosis and fatty infiltration by promoting fibro/adipogenic progenitor apoptosis. PLoS One 2016;11(5):e0155486. [PubMed: 27186977]
9. Davis ME, Korn MA, Gumucio JP, et al. Simvastatin reduces fibrosis and protects against muscle weakness after massive rotator cuff tear. J Shoulder Elbow Surg 2015;24(2):280–287. [PubMed: 25213828]
10. Davis ME, Stafford PL, Jergenson MJ, Bedi A, Mendias CL. Muscle fibers are injured at the time of acute and chronic rotator cuff repair. Clin Orthop Relat Res 2015;473(1):226–232. [PubMed: 25113269]
11. Dellavalle A, Maroli G, Covarello D, et al. Pericytes resident in postnatal skeletal muscle differentiate into muscle fibres and generate satellite cells. Nat Commun 2011;2:499. [PubMed: 21988915]
12. Deniz G, Kose O, Tugay A, Guler F, Turan A. Fatty degeneration and atrophy of the rotator cuff muscles after arthroscopic repair: does it improve, halt or deteriorate? Arch Orthop Trauma Surg 2014;134(7): 985–990. [PubMed: 24845686]
13. Ditsios K, Boutsiadis A, Kapoukranidou D, et al. Chronic massive rotator cuff tear in rats: in vivo evaluation of muscle force and three-dimensional histologic analysis. J Shoulder Elbow Surg 2014;23(12):1822–1830. [PubMed: 24981552]
14. Dunn WR, Schackman BR, Walsh C, et al. Variation in orthopaedic surgeons' perceptions about the indications for rotator cuff surgery. J Bone Joint Surg Am 2005;87(9):1978–1984. [PubMed: 16140812]
15. Fabis J, Danilewicz M, Zwierzchowski JT, Niedzielski K. Atrophy of type I and II muscle fibers is reversible in the case of grade .2 fatty degeneration of the supraspinatus muscle: an experimental study in rabbits. J Shoulder Elbow Surg 2016;25(3):487–492. [PubMed: 26549862]
16. Fabis J, Kordek P, Bogucki A, Mazanowska-Gajdowicz J. Function of the rabbit supraspinatus muscle after large detachment of its tendon: 6-week, 3-month, and 6-month observation. J Shoulder Elbow Surg 2000;9(3):211–216. [PubMed: 10888165]
17. Gerber C, Fuchs B, Hodler J. The results of repair of massive tears of the rotator cuff. J Bone Joint Surg Am 2000;82(4):505–515. [PubMed: 10761941]
18. Gerber C, Meyer DC, Fluck M, Benn MC, von Rechenberg B, Wieser K. Anabolic steroids reduce muscle degeneration associated with rotator cuff tendon release in sheep. Am J Sports Med 2015; 43(10):2393–2400. [PubMed: 26304962]
19. Gerber C, Schneeberger AG, Hoppeler H, Meyer DC. Correlation of atrophy and fatty infiltration on strength and integrity of rotator cuff repairs: a study in thirteen patients. J Shoulder Elbow Surg 2007; 16(6):691–696. [PubMed: 17931904]
20. Gibbons MC, Singh A, Anakwenze O, et al. Histological evidence of muscle degeneration in advanced human rotator cuff disease. J Bone Joint Surg Am 2017;99(3):190–199. [PubMed: 28145949]
21. Gillies AR, Lieber RL. Structure and function of the skeletal muscle extracellular matrix. Muscle Nerve 2011;44(3):318–331. [PubMed: 21949456]
22. Gimbel JA, Van Kleunen JP, Lake SP, Williams GR, Soslowsky LJ. The role of repair tension on tendon to bone healing in an animal model of chronic rotator cuff tears. J Biomech 2007;40(3): 561–568. [PubMed: 16600252]
23. Gladstone JN, Bishop JY, Lo IK, Flatow EL. Fatty infiltration and atrophy of the rotator cuff do not improve after rotator cuff repair and correlate with poor functional outcome. Am J Sports Med 2007;35(5):719–728. [PubMed: 17337727]
24. Gumucio JP, Davis ME, Bradley JR, et al. Rotator cuff tear reduces muscle fiber specific force production and induces macrophage accumulation and autophagy. J Orthop Res 2012;30(12): 1963–1970. [PubMed: 22696414]
25. Gumucio JP, Flood MD, Bedi A, Kramer HF, Russell AJ, Mendias CL. Inhibition of prolyl 4-hydroxylase decreases muscle fibrosis following chronic rotator cuff tear. Bone Joint Res 2017;6(1):57–65. [PubMed: 28108482]
26. Gumucio JP, Flood MD, Roche SM, et al. Stromal vascular stem cell treatment decreases muscle fibrosis following chronic rotator cuff tear. Int Orthop 2016;40(4):759–764. [PubMed: 26224616]

27. Hamano N, Yamamoto A, Shitara H, et al. Does successful rotator cuff repair improve muscle atrophy and fatty infiltration of the rotator cuff? A retrospective magnetic resonance imaging study performed shortly after surgery as a reference. J Shoulder Elbow Surg 2017;26(6):967–974. [PubMed: 28214172]
28. Hosoyama T, Ishiguro N, Yamanouchi K, Nishihara M. Degenerative muscle fiber accelerates adipogenesis of intramuscular cells via RhoA signaling pathway. Differentiation 2009;77(4):350–359. [PubMed: 19281783]
29. Hsu HC, Boardman ND, 3rd, Luo ZP, An KN. Tendon-defect and muscle-unloaded models for relating a rotator cuff tear to glenohumeral stability. J Orthop Res 2000;18(6):952–958. [PubMed: 11192256]
30. Huang AH, Lu HH, Schweitzer R. Molecular regulation of tendon cell fate during development. J Orthop Res 2015;33(6):800–812. [PubMed: 25664867]
31. Jamali AA, Afshar P, Abrams RA, Lieber RL. Skeletal muscle response to tenotomy. Muscle Nerve 2000;23(6):851–862. [PubMed: 10842260]
32. Jo CH, Kim JE, Yoon KS, et al. Does platelet-rich plasma accelerate recovery after rotator cuff repair? A prospective cohort study. Am J Sports Med 2011;39(10):2082–2090. [PubMed: 21737832]
33. Kronberg M, Nemeth G, Brostrom LA. Muscle activity and coordination in the normal shoulder: an electromyographic study. Clin Orthop Relat Res 1990;257:76–85.
34. Lamounier-Zepter V, Ehrhart-Bornstein M, Karczewski P, Haase H, Bornstein SR, Morano I. Human adipocytes attenuate cardiomyocyte contraction: characterization of an adipocyte-derived negative inotropic activity. FASEB J 2006;20(10):1653–1659. [PubMed: 16873888]
35. Laurens C, Louche K, Sengenes C, et al. Adipogenic progenitors from obese human skeletal muscle give rise to functional white adipocytes that contribute to insulin resistance. Int J Obes (Lond) 2016;40(3):497–506. [PubMed: 26395744]
36. Lieber RL, Ward SR. Cellular mechanisms of tissue fibrosis: 4. Structural and functional consequences of skeletal muscle fibrosis. Am J Physiol Cell Physiol 2013;305(3):C241–C252. [PubMed: 23761627]
37. Liu X, Manzano G, Kim HT, Feeley BT. A rat model of massive rotator cuff tears. J Orthop Res 2011;29(4):588–595. [PubMed: 20949443]
38. Liu X, Ning AY, Chang NC, et al. Investigating the cellular origin of rotator cuff muscle fatty infiltration and fibrosis after injury. Muscles Ligaments Tendons J 2016;6(1):6–15. [PubMed: 27331027]
39. Meyer DC, Gerber C, Von Rechenberg B, Wirth SH, Farshad M. Amplitude and strength of muscle contraction are reduced in experimental tears of the rotator cuff. Am J Sports Med 2011;39(7):1456–1461. [PubMed: 21350068]
40. Morag Y, Jacobson JA, Miller B, De Maeseneer M, Girish G, Jamadar D. MR imaging of rotator cuff injury: what the clinician needs to know. Radiographics 2006;26(4):1045–1065. [PubMed: 16844931]
41. Oh M, Nor JE. The perivascular niche and self-renewal of stem cells. Front Physiol 2015;6:367. [PubMed: 26696901]
42. Patel TJ, Lieber RL. Force transmission in skeletal muscle: from actomyosin to external tendons. Exerc Sport Sci Rev 1997;25:321–363. [PubMed: 9213097]
43. Pellegrinelli V, Rouault C, Rodriguez-Cuenca S, et al. Human adipocytes induce inflammation and atrophy in muscle cells during obesity. Diabetes 2015;64(9):3121–3134. [PubMed: 25695947]
44. Randelli P, Menon A, Ragone V, et al. Effects of the pulsed electromagnetic field PST(R) on human tendon stem cells: a controlled laboratory study. BMC Complement Altern Med 2016;16:293. [PubMed: 27538432]
45. Rowshan K, Hadley S, Pham K, Caiozzo V, Lee TQ, Gupta R. Development of fatty atrophy after neurologic and rotator cuff injuries in an animal model of rotator cuff pathology. J Bone Joint Surg Am 2010;92(13):2270–2278. [PubMed: 20926720]
46. Rubino LJ, Stills HF, Jr, Sprott DC, Crosby LA. Fatty infiltration of the torn rotator cuff worsens over time in a rabbit model. Arthroscopy 2007;23(7):717–722. [PubMed: 17637406]

47. Sato EJ, Killian ML, Choi AJ, et al. Skeletal muscle fibrosis and stiffness increase after rotator cuff tendon injury and neuromuscular compromise in a rat model. J Orthop Res 2014;32(9):1111–1116. [PubMed: 24838823]
48. Schmutz S, Fuchs T, Regenfelder F, Steinmann P, Zumstein M, Fuchs B. Expression of atrophy mRNA relates to tendon tear size in supraspinatus muscle. Clin Orthop Relat Res 2009;467(2): 457–464. [PubMed: 18941855]
49. Shirasawa H, Matsumura N, Shimoda M, et al. Inhibition of PDGFR signaling prevents muscular fatty infiltration after rotator cuff tear in mice. Sci Rep 2017;7:41552. [PubMed: 28139720]
50. Steinbacher P, Tauber M, Kogler S, Stoiber W, Resch H, Sanger AM. Effects of rotator cuff ruptures on the cellular and intracellular composition of the human supraspinatus muscle. Tissue Cell 2010; 42(1):37–41. [PubMed: 19709709]
51. Su WR, Budoff JE, Luo ZP. Posterosuperior displacement due to rotator cuff tears. Arthroscopy 2011;27(11):1472–1477. [PubMed: 21908156]
52. Takagishi K, Saitoh A, Tonegawa M, Ikeda T, Itoman M. Isolated paralysis of the infraspinatus muscle. J Bone Joint Surg Br 1994; 76(4):584–587. [PubMed: 8027145]
53. Takegahara Y, Yamanouchi K, Nakamura K, Nakano S, Nishihara M. Myotube formation is affected by adipogenic lineage cells in a cell-to-cell contact-independent manner. Exp Cell Res 2014;324(1): 105–114. [PubMed: 24720912]
54. Trudel G, Ryan SE, Rakhra K, Uhthoff HK. Extra- and intramuscular fat accumulation early after rabbit supraspinatus tendon division: depiction with CT. Radiology 2010;255(2):434–441. [PubMed: 20413756]
55. Uhthoff HK, Coletta E, Trudel G. Intramuscular fat accumulation and muscle atrophy in the absence of muscle retraction. Bone Joint Res 2014;3(4):117–122. [PubMed: 24743593]
56. Uhthoff HK, Matsumoto F, Trudel G, Himori K. Early reattachment does not reverse atrophy and fat accumulation of the supraspinatus—an experimental study in rabbits. J Orthop Res 2003;21(3): 386–392. [PubMed: 12706009]
57. Valencia AP, Iyer SR, Pratt SJ, Gilotra MN, Lovering RM. A method to test contractility of the supraspinatus muscle in mouse, rat, and rabbit. J Appl Physiol (1985) 2016;120(3):310–317. [PubMed: 26586911]
58. Warth RJ, Dornan GJ, James EW, Horan MP, Millett PJ. Clinical and structural outcomes after arthroscopic repair of full-thickness rotator cuff tears with and without platelet-rich product supplementation: a meta-analysis and meta-regression. Arthroscopy 2015;31(2):306–320. [PubMed: 25450417]
59. Yao Y, Norris EH, Mason CE, Strickland S. Laminin regulates PDGFRbeta(1) cell stemness and muscle development. Nat Commun 2016;7:11415. [PubMed: 27138650]
60. Zheng B, Cao B, Crisan M, et al. Prospective identification of myogenic endothelial cells in human skeletal muscle. Nat Biotechnol 2007;25(9):1025–1034. [PubMed: 17767154]

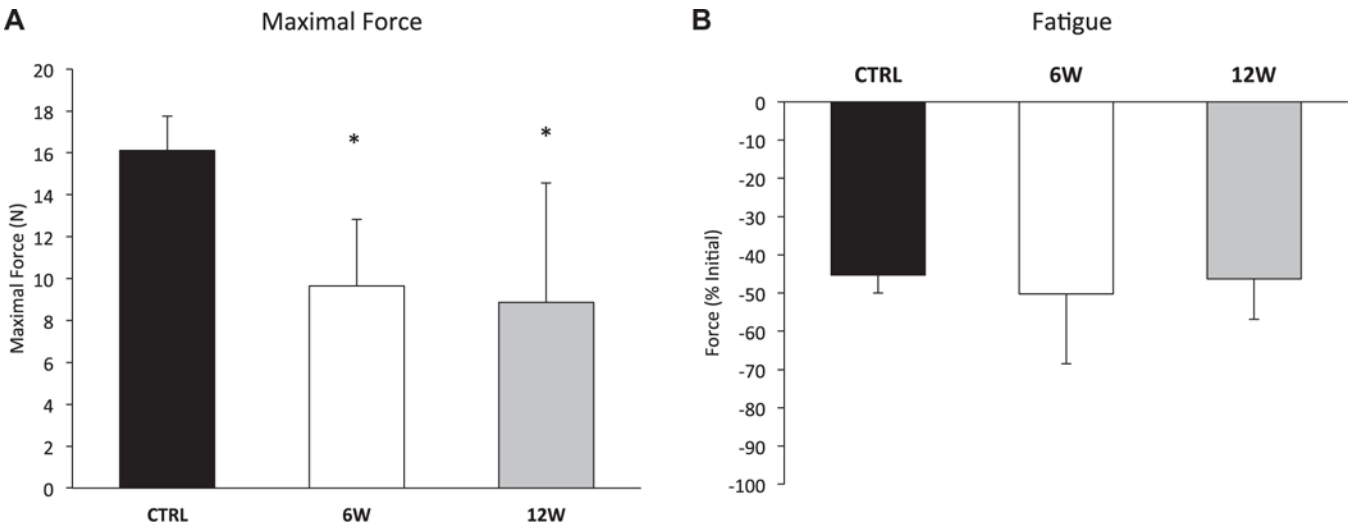


**Figure 1.**

Maximal isometric force is lower at 6 and 12 weeks after rotator cuff tear (RCT). (A) Compared with control, the mean maximal isometric force of the supraspinatus muscle was 40% lower at 6 and 12 weeks after tenotomy, with no differences between these time points. (B) The percentage loss of force (ie, fatigue) was not different among the 3 groups. All values are expressed as mean ± SD. **P* < .05 vs control. n = 5–7 per group. 6W, 6 weeks; 12W, 12 weeks; CTRL, control.

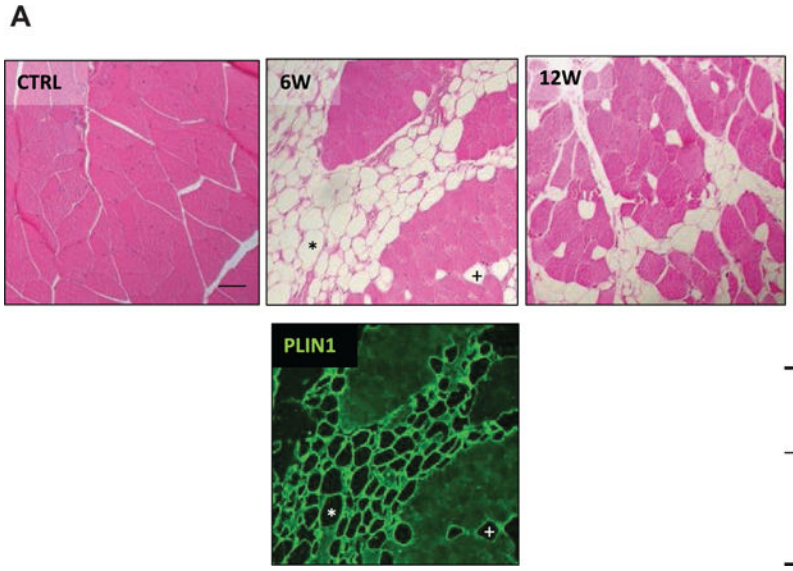


| Location of adipocytes (% adipose area) | 6W | 12W |
|---|---|---|
| PERIFASCICULAR (*) | 75.5 ± 17.4 | 83.1 ± 11.4 |
| INTRAFASCICULAR (+) | 19.0 ± 17.0 | 16.9 ± 11.4 |

**Figure 2.**

Histological assessment of fatty infiltration (FI) after rotator cuff tear. (A) Representative images of FI in the tenotomized muscle (viewed under 20× magnification). The presence of adipocytes in the perifascicular (*) and intrafascicular space (+) (6W image) was confirmed by labeling adipocyte-specific protein perilipin 1 (Plin1) in serial sections. (B) *Top*: Adipocytes covered an average of 9% of the total area of section (% FI) and did not differ between the time points after tenotomy. *Bottom*: About 79% of the adipocytes were in the perifascicular space, and the remaining adipocytes were found in the intrafascicular space, within muscle bundles. Scale bar represents 100 mm. All values are expressed as mean ± SD. *$P < .05$ vs control. n = 5–7 per group. 6W, 6 weeks; 12W, 12 weeks; CTRL, control.

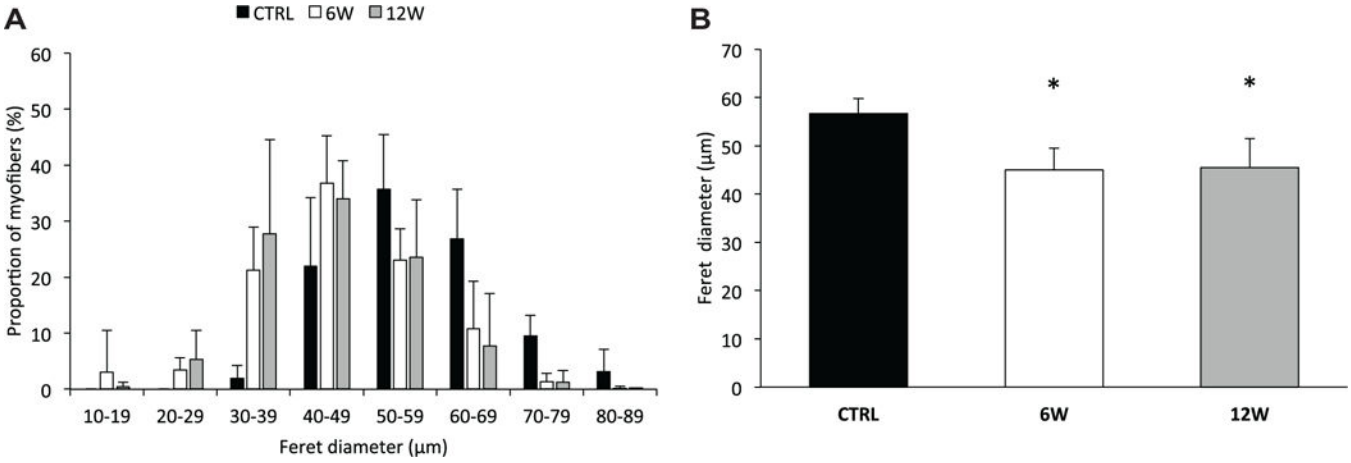


**Figure 3.**

Histological assessment of myofiber size after rotator cuff tear. (A) Minimal Feret diameter of 100 fibers per muscle was measured. Myofibers were binned according to their diameter to determine heterogeneity and shift in myofiber size. There was a larger proportion of smaller myofibers at both time points after tenotomy. (B) The mean diameter was 22% lower in tenotomized muscles versus control, and no differences were detected between the time points. All values are expressed as mean ± SD. *$P < .05$ vs control. n = 5–7 per group. 6W, 6 weeks; 12W, 12 weeks; CTRL, control.

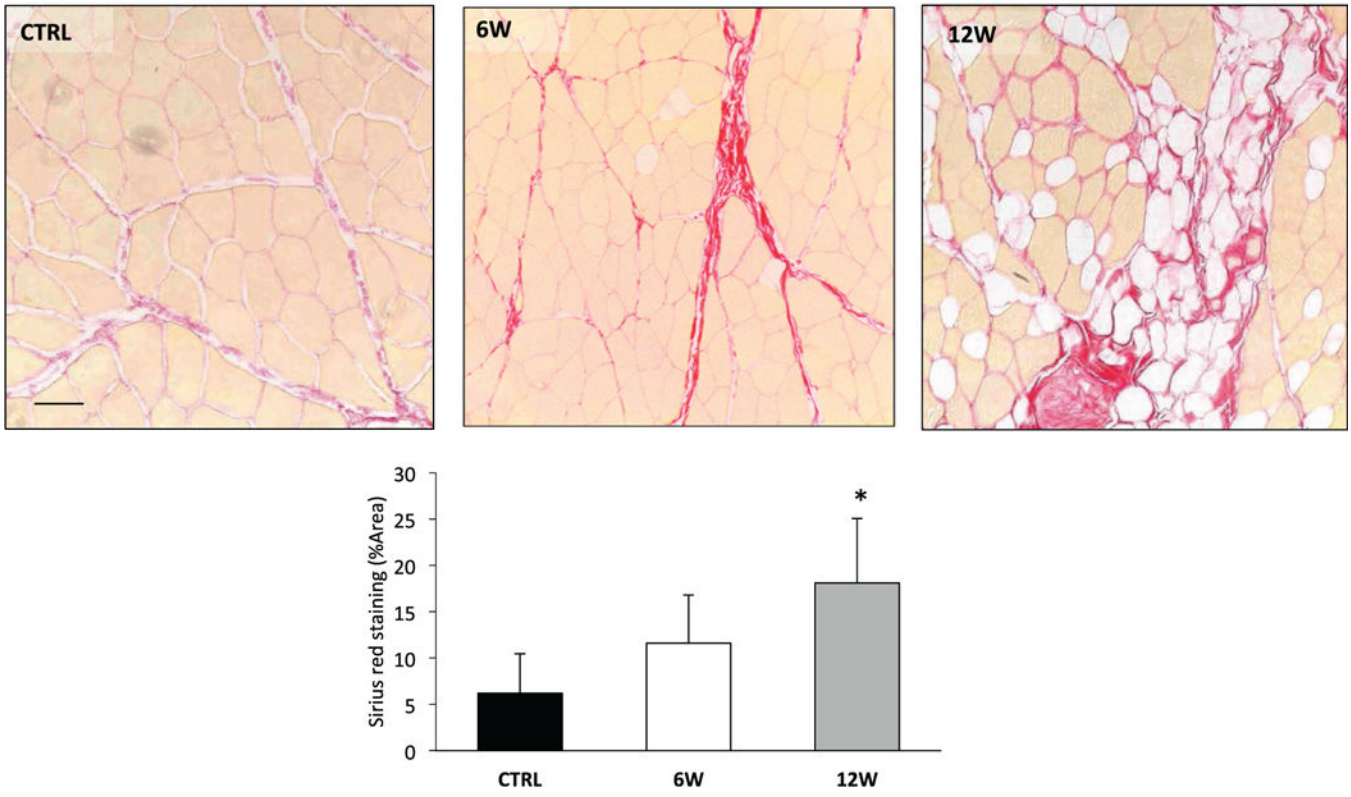


**Figure 4.**

Histological assessment of fibrosis after rotator cuff tear. Collagen content was visualized with Picrosirius red staining. Representative images show specific fields of view (20×) showing collagen staining. Collagen covered 6% of the tissue area in control muscles and 18% in muscles after 12 weeks of tenotomy. No significant differences were found at 6 weeks. Scale bar represents 50 μm. All data are presented as mean ± SD. **P* < .05 vs control. n = 5–7 per group. 6W, 6 weeks; 12W, 12 weeks; CTRL, control.

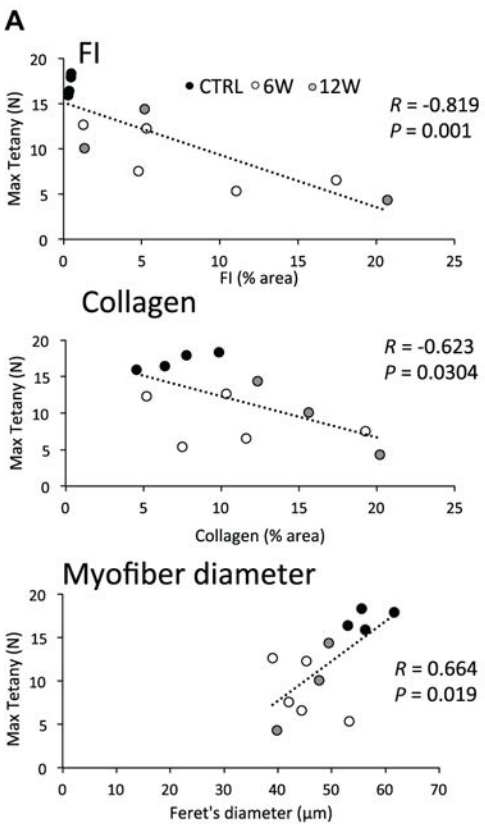


B

| Predictor | β Coefficient | SE | *P* - value |
|---|---|---|---|
| FI (% area) | -0.607 | 13.98 | **0.015** |
| Collagen (% area) | -0.177 | 19.91 | **0.438** |
| Myofiber diameter (μm) | 0.258 | 0.075 | **0.272** |

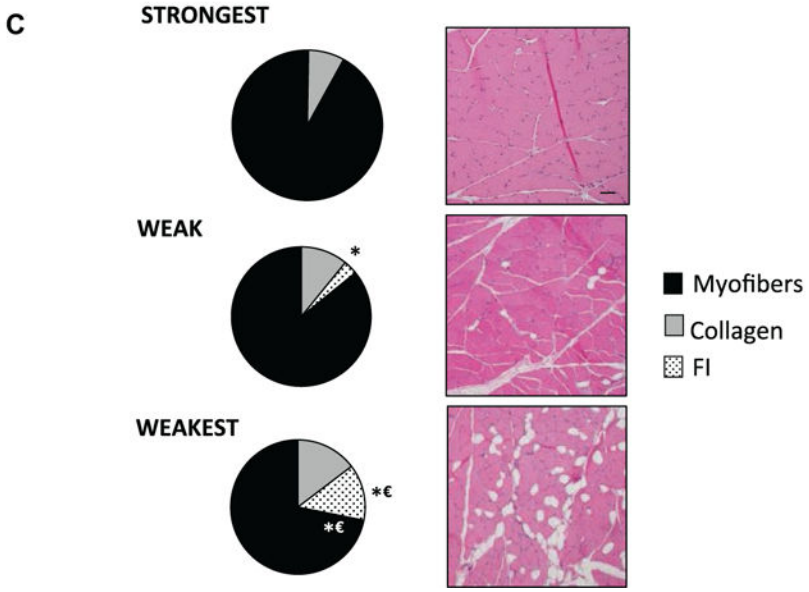


**Figure 5.**

Correlation of histological markers for fatty infiltration (FI), myofiber size, and fibrosis to contractile function of supraspinatus muscle. (A) Pearson correlation analysis to determine the association between maximal isometric force and histological markers shows a significant positive correlation with degree of FI, a moderate negative correlation with collagen, and moderate positive correlation with myofiber size (n = 12). (B) Stepwise multiple linear regression analysis with maximal force as the dependent variable and each histological marker as an independent variable. The histological marker for FI was the strongest predictor of muscle function. (C) Histological characteristics of muscle according to maximal force generated. The strongest third of muscles were compared with those of the middle (weak) and lowest (weakest) third. *Left*: The mean proportions of area covered by FI, collagen, and myofibers in a histological section (n = 4 per group). Compared with the strongest cohort, weaker muscles had FI, and the weakest muscles had the most FI and a smaller area covered by myofibers. *Right*: Representative hematoxylin and eosin images (10×) for each group. Scale bar represents 50 μm. *R* represents the correlation coefficient. **P* < .05 vs control. €*P* < .05 vs weak. 6W, 6 weeks; 12W, 12 weeks; CTRL, control.

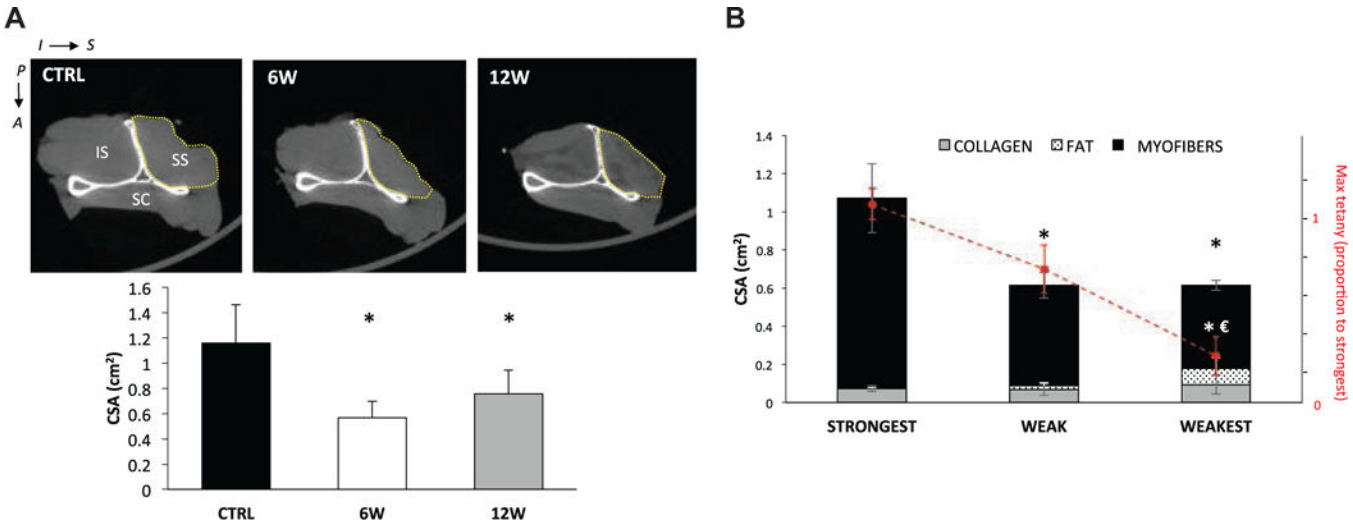


**Figure 6.**

Cross-sectional area (CSA) of the supraspinatus is reduced after rotator cuff tear, and the amount of fatty infiltration (FI) in the muscle is greatest in the weakest muscles. (A) Representative sagittal computed tomography scans of rabbit rotator cuff from control 6 weeks and 12 weeks after tenotomy. The supraspinatus CSA (outlined) was quantified for each group and was lower in animals with rotator cuff tenotomy lasting 6 and 12 weeks. (B) The mean total area of collagen, FI, and myofibers was calculated for the strongest, weak, and weakest muscles. The dashed line indicates the mean force in each cohort as the proportion to the strongest cohort. Compared with the strongest cohort, weak muscles had a smaller total area covered by myofibers that accounted for the decrease in force; however, the weakest cohort did not have a significant decrease in area covered by myofibers to account for its loss in force and was characterized by significant FI (n = 4 per group). All values are expressed as mean ± SD. *R* represents the correlation coefficient. **P* < .05 vs control (A) or strongest (C). €*P* < .05 vs weak. 6W, 6 weeks; 12W, 12 weeks; A, anterior; CTRL, control; I, inferior; IS, infraspinatus; P, posterior; S, superior; SC, subscapularis; SS, supraspinatus.